

Isoscalar and Isovector spin response in sd -shell nuclei

H. Sagawa^{1,2)}, T. Suzuki^{3,4)},

¹⁾*RIKEN, Nishina Center, Wako, 351-0198, Japan*

²⁾*Center for Mathematics and Physics,
University of Aizu, Aizu-Wakamatsu,
Fukushima 965-8560, Japan*

³⁾*Department of Physics,
College of Humanities and Science,
Nihon University, Sakurajosui 3,
Setagaya-ku, Tokyo 156-8550, Japan*

⁴⁾*National Astronomical Observatory of Japan,
Mitaka, Tokyo 181-8588, Japan*

The spin magnetic dipole transitions and the neutron-proton spin-spin correlations in sd -shell even-even nuclei with $N = Z$ are investigated using shell model wave functions taking into account enhanced isoscalar (IS) spin-triplet pairing as well as the effective spin operators. It was shown that the IS pairing and the effective spin operators gives a large quenching effect on the IV spin transitions to be consistent with observed data by (p, p') experiments. On the other hand, the observed IS spin strength show much smaller quenching effect than expected by the calculated results. The IS pairing gives a substantial quenching effect on the spin magnetic dipole transitions, especially on the isovector (IV) ones. Consequently, an enhanced isoscalar spin-triplet pairing interaction enlarges the proton-neutron spin-spin correlation deduced from the difference between the isoscalar (IS) and the IV sum rule strengths. The beta-decay rates and the IS magnetic moments of sd -shell are also examined in terms of the IS pairing as well as the effective spin operators.

PACS numbers: 21.60.Jz, 21.65.Ef, 24.30.Cz, 24.30.Gd

I. INTRODUCTION

The spin-isospin response is a fundamental process in nuclear physics and astrophysics. The Gamow-Teller (GT) transition, which is a well-known "allowed" charge exchange transition, involves the transfer of one unit of the total angular momentum induced by $\vec{\sigma}t_{\pm}$ [1]. In a no-charge-exchange channel, magnetic dipole (M1) transitions are extensively observed in a broad region of the mass table. Both the spin and the angular momentum operators induce M1 transitions [1], and depending on whether the isospin operator is included also induce the isovector (IV) and the isoscalar (IS) modes.

Compared to the relevant theoretical predictions by shell model and random phase approximations (RPA) [2–7], the experimental rates of these spin-isospin responses are quenched. A similar quenching effect also occurs in the observed magnetic moments of almost all nuclei compared to the single-particle unit (i.e., the Schmidt value) [1, 8, 9]. The quenching effect of spin-isospin excitations influences many astrophysical processes such as the mean free path of neutrinos in dense neutron matter, the dynamics and nucleosynthesis in core-collapse supernovae explosions [10], and the cooling of protoneutron stars [11]. Furthermore, the exhaustion of the GT sum rule is directly related to the spin susceptibility of asymmetric nuclear matter [12] and the spin-response to strong magnetic fields in magnetars [13].

Although the quenching phenomena of magnetic moments and spin responses have been extensively studied,

previous research has focused mainly on the mixings of higher particle-hole (p-h) configurations [8, 9, 14] and the coupling to the Δ resonances [15, 16]. In particular, the measured strength of the GT transitions up to the GT giant resonance is strongly quenched compared to the non-energy weighted sum rule, $3(N - Z)$ [2]. This observation has raised a serious question about standard nuclear models because the sum rule is independent of the details of the nuclear model, implying a strong coupling to Δ . After a long debate [17], experimental investigations by charge-exchange (p, n) and (n, p) reactions on ^{90}Zr using multipole decomposition (MD) techniques have revealed about 90% of the GT sum rule strength in the energy region below $E_x=50$ MeV [4, 18], demonstrating the significance of the $2p - 2h$ configuration mixings due to the central and tensor forces [14], although the coupling to Δ is not completely excluded.

IV spin M1 transitions induced by $\vec{\sigma}t_z$ can be regarded as analogous to GT transitions between the same combination of the isospin multiplets. Therefore, they should show the same quenching effect as GT transitions. On the other hand, the IS spin M1 transitions are free from the coupling to Δ and their strength quenching should be due to higher particle-hole configurations. Various theoretical studies have pointed out that the quenching of IS spin operators is similar to that of IV ones [19]. However, recent high-resolution proton inelastic scattering measurements at $E_p=295$ MeV have revealed that the IS quenching is substantially smaller than the IV quenching for several $N=Z$ sd -shell nuclei [20]. These empirical findings give rise to a positive value for the proton-

neutron spin-spin correlations in the ground state of $N=Z$ nuclei.

Recently, it has been reported that the isoscalar (IS) spin-triplet pairing correlations play an important role in enhancing the GT strength near the ground states of daughter nuclei with mass $N \sim Z$ [21–24]. At the same time, the total sum rule of the GT strength is quenched by ground state correlations due to the IS pairing [25].

In this paper, we study the IS and IV spin M1 responses based on modern shell model effective interactions for the same set of $N=Z$ nuclei as those in Ref. [20]. We introduce effective spin and spin-isospin operators to make quantitative study of the accumulated strength in the responses. We consider that simultaneous calculations of these responses within the same nuclear model may be advantageous to distinguish the effect of the higher order configurations from the Δ -hole coupling due to the fact that the IS spin M1 transition is independent of the Δ -hole coupling strength. We discuss also the effect of IS spin-triplet pairing interaction on the spin responses and the proton-neutron spin-spin correlations in the ground states of $N=Z$ nuclei.

The spin M1 operators are introduced in Section II and their sum rules are also defined. Section III is devoted to the shell model calculations of $N=Z$ even-even nuclei in comparisons with available experimental data by (p, p') reactions. The accumulated sum rule values of IS and IV spin transitions are extracted in Section 4. The proton-neutron spin-spin correlations are also discussed in terms of the IS spin-triplet pairing correlations. The beta-decay rates and IS magnetic moments in sd -shell are studied in the same context of the shell model calculations in Section V. The summary is given in Section VI.

II. SPIN M1 OPERATORS AND SUM RULES

We consider the IS and IV spin M1 operators, which are given as

$$\hat{O}_{IS} = \sum_i \vec{\sigma}(i), \quad (1)$$

$$\hat{O}_{IV} = \sum_i \vec{\sigma}(i)\tau_z(i), \quad (2)$$

as well as the GT charge exchange excitation operators, which is expressed as

$$\hat{O}_{GT} = \sum_i \vec{\sigma}(i)t_{\pm}(i). \quad (3)$$

The sum rule values for the M1 spin transitions are defined by

$$S(\vec{\sigma}) = \sum_f \frac{1}{2J_i + 1} |\langle J_f || \hat{O}_{IS} || J_i \rangle|^2, \quad (4)$$

$$S(\vec{\sigma}\tau_z) = \sum_f \frac{1}{2J_i + 1} |\langle J_f || \hat{O}_{IV} || J_i \rangle|^2. \quad (5)$$

For the GT transition, the sum rule value is defined by

$$S(\vec{\sigma}t_{\pm}) = \sum_f \frac{1}{2J_i + 1} |\langle J_f || \hat{O}_{GT} || J_i \rangle|^2, \quad (6)$$

and satisfies the model independent sum rule,

$$S(\vec{\sigma}t_-) - S(\vec{\sigma}t_+) = 3(N - Z). \quad (7)$$

According to Ref. [20], the proton-neutron spin-spin correlation is defined as

$$\begin{aligned} \Delta_{spin} &= \frac{1}{16} (S(\vec{\sigma}) - S(\vec{\sigma}\tau_z)) \\ &= \sum_f \langle J_i | \sum_i \frac{\vec{\sigma}_n(i) + \vec{\sigma}_p(i)}{4} | J_f \rangle \langle J_f | \sum_i \frac{\vec{\sigma}_n(i) + \vec{\sigma}_p(i)}{4} | J_i \rangle \\ &\quad - \sum_f \langle J_i | \sum_i \frac{\vec{\sigma}_n(i) - \vec{\sigma}_p(i)}{4} | J_f \rangle \langle J_f | \sum_i \frac{\vec{\sigma}_n(i) - \vec{\sigma}_p(i)}{4} | J_i \rangle \\ &= \langle J_i | \vec{S}_p \cdot \vec{S}_n | J_i \rangle, \end{aligned} \quad (8)$$

where $\vec{S}_p = \sum_{i \in p} \vec{\sigma}_p(i)$ and $\vec{S}_n = \sum_{i \in n} \vec{\sigma}_n(i)$. The correlation value is 0.25 and -0.75 for a proton-neutron pair with a pure spin triplet and a singlet, respectively. The former corresponds to the ferromagnet limit of the spin alignment, while the latter is the anti-ferromagnetic one.

III. SHELL MODEL CALCULATIONS WITH EFFECTIVE OPERATORS AND IS PAIRING CORRELATIONS

The shell model calculations are performed in full sd -shell model space with the USDB interaction [26]. Among the effective interactions of the USD family, USD [27], USDA [26], and USDB [26], the results of spin excitations with $J^{\pi}=1^+$ are quite similar to each other both in excitation energies and transition strengths for collective states with large transition strengths. Hereafter, we present results based on USDB interaction. To take into account the effects of higher order configuration mixings as well as meson exchange currents (MEC) and Δ -isobar effect, effective operators are commonly adopted in the study of magnetic moments, GT transitions and spin and spin-isospin dependent β -decays.

IV magnetic transitions in sd -shell nuclei and GT transitions have been studied extensively in experiments and theories. On the other hand, experimental evidence of IS magnetic transitions are not well known so far except recent experimental data by Matsubara et al.. In the literature [8, 9, 28], the effective operators have been introduced to mimic the effects of higher-order configuration mixings, meson-exchange currents, Δ -isobar coupling and the relativistic corrections. For the spin operators, the effective operators read for the IS operator

$$\hat{O}_{IS}^{eff} = f_s^{IS} \vec{\sigma} + f_l^{IS} \vec{l} + f_p^{IS} \sqrt{8\pi} [Y_2 \times \vec{\sigma}]^{(\lambda=1)} \quad (9)$$

and also for the IV spin operator,

$$\hat{O}_{IV}^{eff} = f_s^{IV} \vec{\sigma}\tau_z + f_l^{IV} \vec{l}\tau_z + f_p^{IV} \sqrt{8\pi} [Y_2 \times \vec{\sigma}]^{(\lambda=1)} \tau_z \quad (10)$$

where $f_i^{IS(IV)}$ ($i = s, l, p$) are the effective coefficients of $IS(IV)$ spin, orbital and spin-tensor operators. The summation of index i in Eq. (1) is discarded in the effective operators. The effective coefficients for the IS spin operator obtained by Towner are $f_s^{IS} = 0.745$, $f_l^{IS} = 0.0526$ and $f_p^{IS} = -0.0157$. For the IV part, Towner obtained the corrections for the spin, orbital and the spin-tensor operators of GT transitions of $1d$ -orbit as

$$\hat{O}_{GT}^{eff} = (1 + \delta g_s) \vec{\sigma} t_{\pm} + \delta g_l \vec{l} t_{\pm} + \delta g_p \sqrt{8\pi} [Y_2 \times \vec{\sigma}]^{(\lambda=1)} t_{\pm} \quad (11)$$

with

$$\delta g_s = -0.139, \quad \delta g_l = 0.0103, \quad \delta g_p = 0.0283 \quad (12)$$

due to the various higher order effects. In the shell model calculations with USD interaction, the IV spin and charge exchange GT excitations are the same features since no isospin breaking interaction such as Coulomb interaction and charge symmetry breaking forces is not included. We adopt the GT effective operators for IV spin transitions. For the isoscalar part, the quenching factor for spin operator is introduced to check the sensitivity of transition strength on the effective operator. The effective operators for IS orbital and spin-tensor are not introduced in the present study. For the IS case, we take 4 different versions of calculations:

- USDB: the original interaction with the bare spin operator
- USDB1: the IS spin-triplet pairing matrix is enhanced multiplying a factor 1.1 on the relevant matrix elements of USDB interaction. The bare spin operator is adopted.
- USDB2: the IS spin-triplet pairing matrix is enhanced multiplying a factor 1.1 on the relevant matrix elements of USDB interaction. The IS spin operator is 10% quenched: $f_s^{IS} = 0.9$.
- USDB3: the IS spin-triplet pairing matrix is enhanced multiplying a factor 1.2 on the relevant matrix elements of USDB interaction. The IS spin operator is 10% quenched: $f_s^{IS} = 0.9$.

For the IV case, we take 3 different cases of calculations:

- USDB: the original interaction with the bare spin operator
- USDBq1: the IS spin-triplet pairing matrix is enhanced multiplying a factor 1.1 on the relevant matrix elements of USDB interaction. The effective IV spin operator is adopted.
- USDBq2: the IS spin-triplet pairing matrix is enhanced multiplying a factor 1.2 on the relevant matrix elements of USDB interaction. The effective IV spin operator is adopted.

A. ^{12}C

In ^{12}C , IS and IV 1^+ states are observed at $Ex=12.71$ and 15.11MeV , respectively. The $B(M1)$ values are extracted from (e, e') scattering experiments to be $B(M1)=0.0402$ and 2.679 in terms of nuclear magneton $(e\hbar/2mc)^2$ [29]. The shell model calculations with CK-POT interaction give $B(M1)=0.01434$ and 2.314 in the unit of nuclear magneton at $Ex=12.45$ and 15.09MeV , respectively, with the bare magnetic transition operators. A recent $p - sd$ shell Hamiltonian, SFO [30], gives $B(M1) = 0.0131$ and $2.515 \mu_N^2$ for the IS and IV transitions, respectively. The model space of SFO is $p - sd$ shell and the excitations from p -shell to sd -shell are included up to $2\hbar\omega$. It is noticed that the experimental value is about 3 times larger than the calculated value for the IS 1^+ state at $Ex=12.71\text{MeV}$, while the calculated value for the IV state is close to the experimental value. The (p, p') data was reported for the two 1^+ states to be $B(\sigma) = 3.174 \pm 0.842$ at $Ex=12.71\text{MeV}$ and $B(\sigma\tau) = 1.909 \pm 0.094$ at $Ex=15.11\text{MeV}$, respectively. The shell model results with SFO are $B(\sigma)=1.516$ and $B(\sigma\tau)=1.937$, respectively. The proton inelastic scattering data of the state at $Ex=12.71\text{MeV}$ show also a factor 2 larger value than the shell model results. The isospin mixing between the two 1^+ state has been discussed as an origin of the enhancement of IS spin matrix element. A large isospin mixing was claimed to enhance IS magnetic transition observed by the electron scattering.

The same effect is expected for $B(\sigma)$. When the 1^+ , $T=0$, 12.71 MeV and 1^+ , $T=1$, 15.11 MeV state are mixed by isospin-mixing,

$$\begin{aligned} |1^+, 12.71 \text{ MeV} \rangle &= \sqrt{1-a^2} |1^+, T=0\rangle + a |1^+, T=1\rangle \\ |1^+, 15.11 \text{ MeV} \rangle &= \sqrt{1-a^2} |1^+, T=1\rangle - a |1^+, T=0\rangle \end{aligned} \quad (13)$$

we get an enhancement of $B(\sigma)$ as well as a reduction of $B(\sigma\tau)$. $B(\sigma)$ is enhanced from 1.516 to 1.714 while $B(\sigma\tau)$ is reduced from 1.937 to 1.750 and the mixing amplitude $a = 0.056$ [31]. The difference Δ_{spin} (Eq. (8)) is found to be enhanced by 0.024 . Though the isospin-mixing gives rise to favorable effects, it is still not enough to reproduce the experimental value of $B(\sigma)$.

B. ^{20}Ne

Figures 1(a) and 2(a) show the energy spectra of the IS spin excitations and their accumulative sums, respectively, in ^{20}Ne . The IS spin-triplet matrix elements are enhanced by a factor 1.1 for USDB1 and USDB2, and by a factor 1.2 for USDB3 case. Together with the enhancement of IS pairing, the quenched spin operator is introduced in the cases USDB2 and USDB3 with $q=0.9$. The calculated results are smoothed by a Lorentzian weighting factor with the width of 0.5 MeV to guide the eye. The shell model results with USDB give 1^+ states at $Ex=12.64$ and 14.98 MeV with $B(\sigma) = 0.360$

and 0.519, respectively. The USDB3 results with the enhanced pairing and the quenched spin operator are also shown in the same figure. The lowest state in the case of USDB3 is found at $Ex=12.55\text{MeV}$ with a smaller strength $B(\sigma) = 0.178$, which is a half of USDB one. The higher energy strength is fragmented into three peaks at $Ex\sim 14.5$ and 16.6 MeV with the summed strength $B(\sigma)=0.19$. The accumulated values are shown in Fig. 2 for four cases USDB, USDB1, USDB2 and USDB3. In ^{20}Ne , the accumulated sum increases up to $Ex\sim 20\text{MeV}$. The enhanced IS pairing in USDB1 gives about 10 % quenching compared with USDB results, while more enhanced IS pairing in USDB3 gives further quenching compared with USDB2. In the (p, p') data, the IS strengths are not found so far.

The results of IV spin response are shown in Figures 1(b) and 2(b). The original USDB gives IV strength at $Ex=11.16$ and 13.49MeV with $B(\sigma\tau)=0.331$ and 0.183 , respectively, below $Ex=15\text{MeV}$. The excitation energies of these two peaks are shifted to higher energies 11.62 and 13.92MeV in the case of enhanced IS pairing USDBq1. Comparing with the results of USDBq1, the USDBq2 gives essentially the same excitation energies for 1^+ spectra, while the $B(\sigma\tau)$ are decreased from 0.292 to 0.230 for the first peak and from 0.113 to 0.0627 for the second peak. The calculated results give large strength also in the energy region above $Ex=15\text{MeV}$. The accumulated sums are shown in Figure 2(b). Up to $Ex=16\text{MeV}$, the accumulated sums are 0.577 , 0.406 and 0.293 for USDB, USDBq1 and USDBq2, respectively. Due to the strong IS pairing and the effective IS spin operator, the accumulated strength decrease by 30% for USDBq1 and 50% for USDBq2. The (p, p') experiments found two IV strength at $Ex = 11.26$ and 13.36MeV with $B(\sigma\tau)=0.369$ and 0.018 , respectively. The summed strength 0.387 is comparable with the result of USDBq1.

C. ^{24}Mg

Figures 3 and 4 show the energy spectra of the spin excitations and their accumulative sums, respectively, in ^{24}Mg . For the IS case, the experimental data give the strong spin M1 strength at $Ex=9.828\text{MeV}$ with $B(\sigma) = 3.886 \pm 1.102$. The shell model results with USDB give IS 1^+ state at $Ex=9.818\text{MeV}$ with $B(\sigma) = 3.278$. In the (p, p') data, other IS strengths are also found at 7.748MeV with $B(\sigma)=0.508$ and at $Ex\sim 14\text{MeV}$ with $B(\sigma) \sim 1.2$. The calculated results reproduce strong M1 states at very similar energies $Ex=7.82$ and 13.7MeV with $B(\sigma) = 0.24$ and 0.59 , respectively. The calculations with USDB show also the same amount of $B(\sigma)$ value as the experimental data around $Ex=14\text{MeV}$. The summed strength up to $Ex=16\text{MeV}$ is $B_{exp}(\sigma; Ex\leq 16\text{MeV})=5.061\pm 1.166$, while the calculated sum is $B_{cal}(\sigma; Ex\leq 16\text{MeV})=4.256$. The calculated results of USDB3 changes only slightly the excitation energies of 1^+ state by about 100-200keV, while

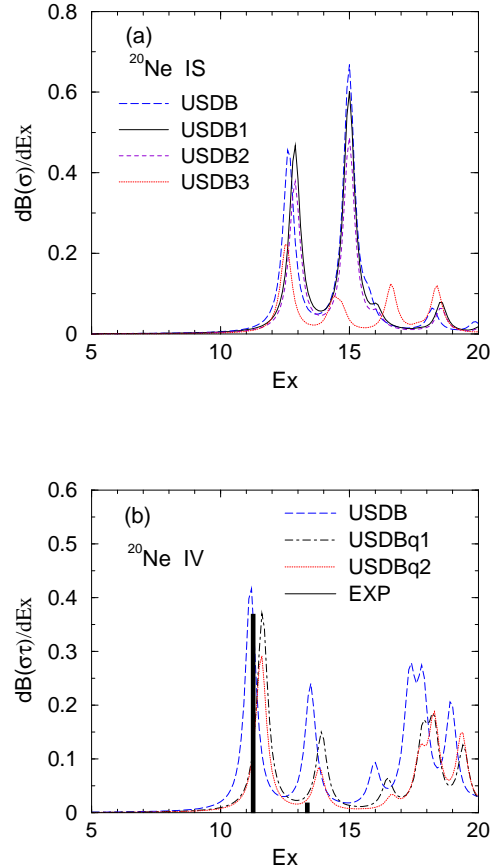


FIG. 1. (Color online) IS (top) and IV spin-M1 (bottom) transition strengths in ^{20}Ne . Shell model calculations are performed in the full sd -shell model space with an USDB effective interaction. For the IS case, the USDB1 and USDB2 has the 10% enhanced IS spin-triplet interaction, while USDB3 has 20% enhanced ones. The quenching factor for the IS spin operator $f_s^{IS}=0.9$ is introduced for USDB2 and USDB3 calculations. For the results of the IV spin-M1 transitions, an effective IV spin operator (11) is adopted in USDBq1 and USDBq2 cases. The IS spin-triplet interaction is enhanced by multiplying the relevant matrix elements by factors 1.1 and 1.2 in the cases of USDBq1 and USDBq2, respectively, together with the effective operator. Calculated results are smoothed by taking a Lorentzian weighting factor with the width of 0.5MeV , while the experimental data are shown in the units of $B(\sigma)$ for the IS excitations and $B(\sigma\tau)$ for the IV excitations. Experimental data are from ref. [20].

the summed $B(\sigma)$ value is decreased by 30% .

The experimental analysis show a strong IV spin strength at $Ex=10.71\text{MeV}$ with $B(\sigma\tau)=1.714$. The calculation gives at $Ex=10.723\text{MeV}$ with $B(\sigma\tau)=1.854$. Experimental data show also substantial strength around $Ex=12.8\text{MeV}$ with $B(\sigma) \sim 1$ and at $Ex=9.968$ and 16.046MeV with $B(\sigma\tau)=0.18$ and 0.29 , respectively. The calculated results give large strengths at $Ex=9.939\text{MeV}$ and 10.75MeV with $B(\sigma\tau)=0.238$ and

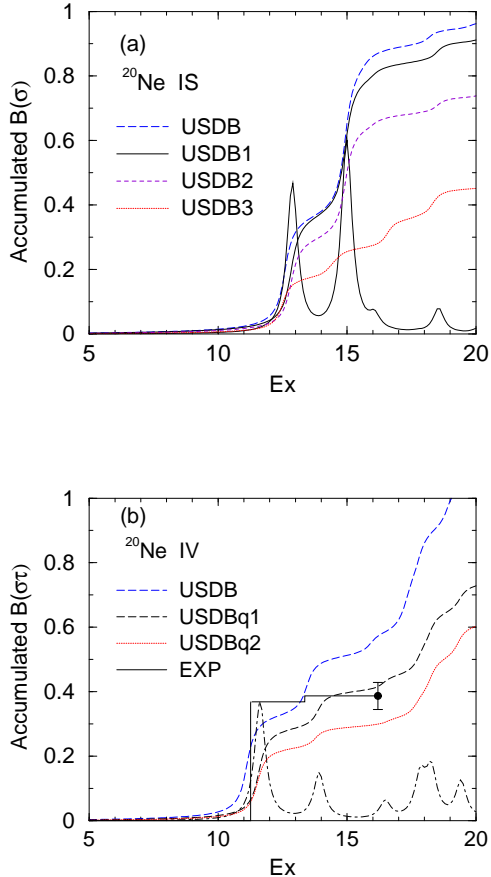


FIG. 2. (Color online) Accumulative sum of the IS spin-M1 strength (top) and the IV spin-M1 strength (bottom) as a function of the excitation energy in ^{20}Ne . The calculated energy spectra are also shown for USDB1 in the IS channel and for USDBq1 in the IV channel. Calculated results are smoothed in the same manner as Fig. 1. Dot with a vertical error bar denotes the experimental accumulated sum of the strengths. See the text and the caption to Fig. 1 for details.

1.521, respectively. The experimental summed strength is $B_{exp}(\sigma\tau; Ex \leq 16\text{MeV}) = 3.180 \pm 0.236$, while the calculated value is $B_{cal}(\sigma\tau; Ex \leq 16\text{MeV}) = 3.855$. There are about 20% quenching in the empirical IV spin sum rule strength below $Ex = 16\text{MeV}$ compared with USDB results with the bare spin operator. The USDBq1 and USDBq2 results with the effective spin operator show about 30 and 40% quenching of the accumulated strength up to $Ex = 16\text{MeV}$, respectively.

We study the effects of the isospin-mixing in ^{24}Mg . The 1^+ , $T=0$ states at $E_x = 7.747\text{ MeV}$ and 9.827 MeV are mixed with the 1^+ , $T=1$ state at $E_x = 9.966\text{ MeV}$ [32]. Using the mixing amplitudes obtained by $\langle T = 1|V_C D|T = 0 \rangle / \Delta E$ with $\langle T = 1|V_C D|T = 0 \rangle = 49\text{ keV}$ [32], an enhancement of $S(\vec{\sigma})$ from 4.256 to 4.492, a reduction of $S(\vec{\sigma}\tau_z)$ from 3.856 to 3.652 and an enhancement of Δ_{spin} by 0.026 are obtained for USDB. These

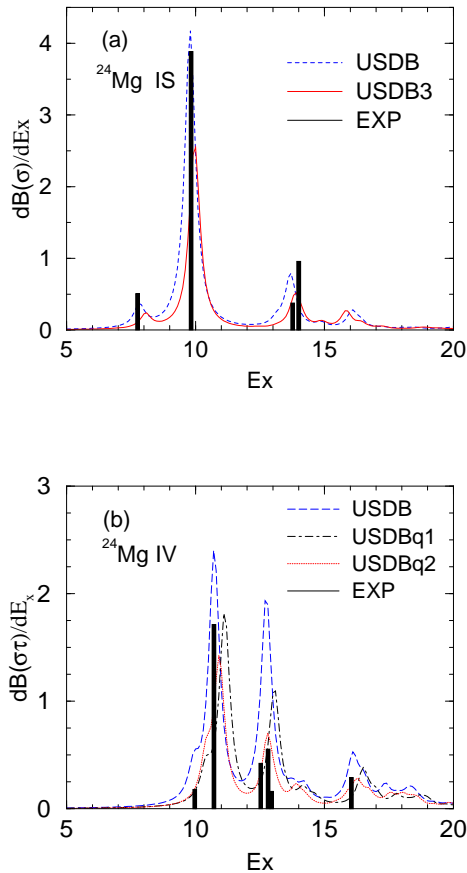


FIG. 3. (Color online) IS (top) and IV spin-M1 (bottom) transition strengths in ^{24}Mg . See the text and the caption to Fig. 1 and the text for details.

effects are favorable and consistent with the experimental data though their magnitudes are not significant.

D. ^{28}Si

The calculated results of IS response are shown in Figs. 5(a) and 6(a). The calculated results give a IS 1^+ state at $Ex = 9.6\text{MeV}$ with USDB interaction, which reproduces well the experimental IS 1^+ state with a strong spin transition at $E_x = 9.58\text{MeV}$ exhausting about 70% of the total IS strength. Another strong state is observed at $Ex = 14.571\text{MeV}$ with $B(\sigma) = 2.075 \pm 0.621$, while the calculation shows no sign of strong $B(\sigma)$ transition above $Ex = 14\text{MeV}$. Other IS spin transitions are found experimentally at $Ex \sim 13\text{MeV}$ with $B(\sigma) \sim 0.7$. The calculations show also the IS spin strength of $B(\sigma) \sim 1.0$ at $Ex = (12.3-13.2)\text{MeV}$. The summed empirical IS strength below $Ex = 16\text{MeV}$ is $B_{exp}(\sigma; Ex \leq 16\text{MeV}) = 6.489 \pm 1.604$, while the calculated results are $B_{cal}(\sigma; Ex \leq 16\text{MeV}) = 6.816, 6.611, 5.355$ and

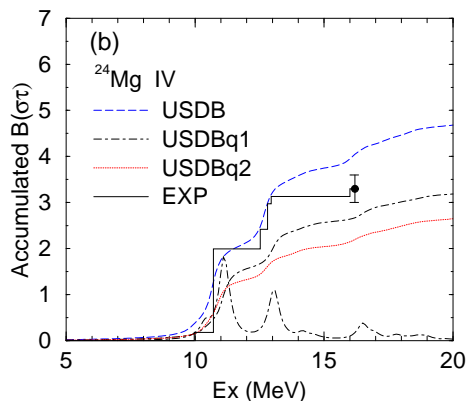
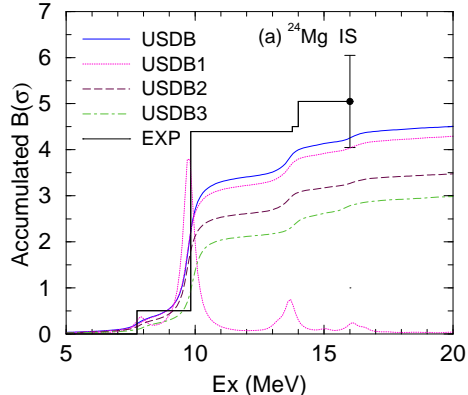


FIG. 4. (Color online) Accumulative sum of the IS spin-M1 strength (top) and the IV spin-M1 strength (bottom) as a function of the excitation energy in ^{24}Mg . See the text and the caption to Fig. 2 and the text for details.

4.562 for USDB, USDB1, USDB2 and USDB3, respectively. The $B_{cal}(\sigma; Ex \leq 16\text{MeV})$ values show 3, 21 and 33% quenching for USDB1, USDB2 and USDB3 interactions, respectively, compared with USDB results.

The IV spin response is shown in Figs. 5(b) and 6(b). Gross structure of empirical IV spin response is well reproduced by the calculations based on USDB interaction. Empirical IV spin strength is rather fragmented, while two IV 1^+ states with strong spin strengths of $B(\sigma\tau)=2.05$ and 0.92 are reported at $E_x=11.45$ and 14.01MeV , respectively. Calculated results show also largely fragmented IV spin strength and two strong strength are found at $Ex=11.48$ and 14.26MeV with $B(\sigma\tau)=2.165$ and 1.773 , respectively, with USDB interaction. The empirical IV summed strength is $B_{exp}(\sigma\tau; Ex \leq 16\text{MeV})=4.59 \pm 0.222$, while the calculated one is $B_{cal}(\sigma\tau; Ex \leq 16\text{MeV})=7.34$, 5.03 and 4.03 for USDB, USDBq1 and USDBq2 cases, respectively. In the spin IV sum rule value, we see a large quenching spin factor $q_s^{IV}(\text{eff}) \equiv \sqrt{B_{exp}(\sigma\tau)/B_{cal}(\sigma\tau : \text{USDB})}=0.79$, which

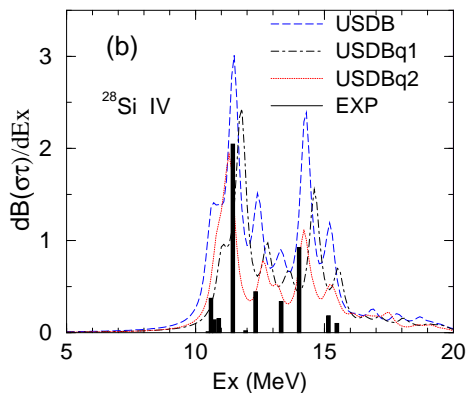
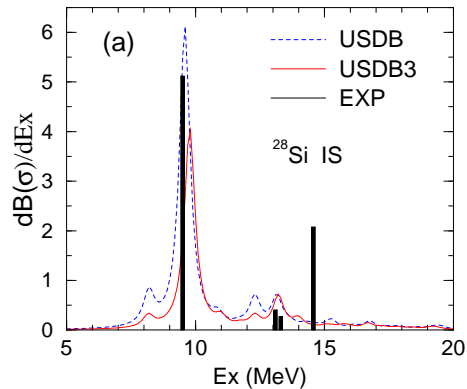


FIG. 5. (Color online) IS (top) and IV spin-M1 (bottom) transition strengths in ^{28}Si . See captions to Fig. 1 and the text for details.

is close to the ratio of summed values of USDBq1 to USDB. It is pointed out also in ref. [33] that the enhanced IS pairing multiplying a factor 1.2 on the IS pairing matrices reduces the IV spin transition strength, corresponding to the renormalization factor of $f_s^{IV}=0.87$ for the accumulated IV spin strength. On the other hand, the same enhanced IS pairing gives the IS quenching factor $f_s^{IS}=0.91$. This difference between IS and IV spin response induces a positive value for the proton-neutron spin-spin correlations in the ground state. This point will be discussed more in Section IV.

E. ^{32}S

For the IS case shown in Fig. 7(a), the experimental data show a strong state at $Ex=9.956\text{MeV}$ with $B(\sigma) = 3.810 \pm 1.118$. The corresponding state is found in the calculated results at $Ex=9.632\text{MeV}$ with $B(\sigma) = 4.312$. Another strong IS transition was found at $Ex=9.297\text{MeV}$ with $B(\sigma) = 1.461 \pm 0.436$, while

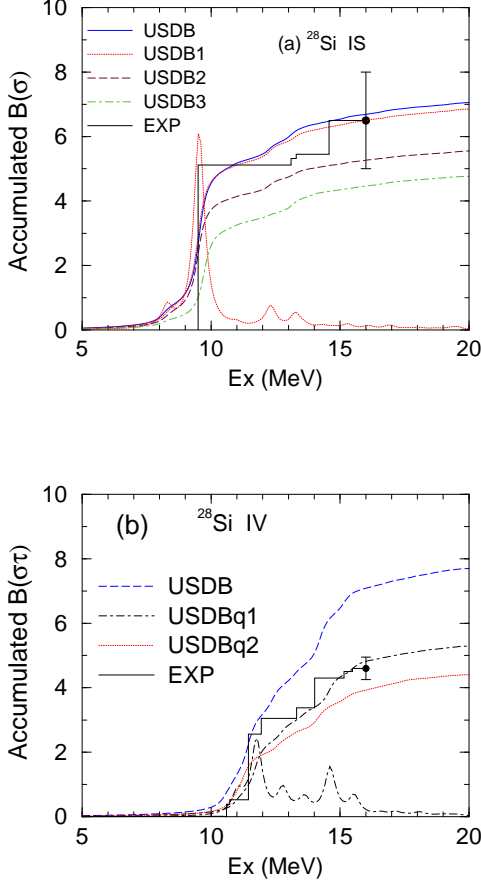


FIG. 6. (Color online) Accumulative sum of the IS spin-M1 strength (top) and the IV spin-M1 strength (bottom) as a function of the excitation energy in ^{28}Si . See the captions to Fig. 2 and the text for details.

the calculations show a state at $Ex=9.154\text{MeV}$ with $B(\sigma) = 1.293\text{MeV}$. There are two IS states observed below $Ex=7.2\text{MeV}$. The calculations found also two states at the same energy region with almost the same $B(\sigma)$ values as the observed ones. The observed IS sum rule strength is $B_{exp}(\sigma:Ex \leq 16\text{MeV}) = 6.414 \pm 1.227$, while theoretically $B_{cal}(\sigma:Ex \leq 16\text{MeV}) = 7.623$. We can see a small quenching effect corresponding to $f_s^{IS}(eff) = 0.92$ for the sum rule strength below $Ex=16\text{MeV}$.

The IV response in ^{32}S is shown Fig. 7(b). The IV spin strength is concentrated at $Ex \sim 11.3\text{MeV}$ having 80% of the total strength below $Ex=16\text{MeV}$. The calculated results show also very large fraction of the total strength of about 87% of the total strength. Another strong state is found experimentally at $Ex=8.125\text{MeV}$ with $B(\sigma\tau) = 0.730 \pm 0.040$, while the calculations show a state at $Ex=7.959\text{MeV}$ with $B(\sigma\tau)=0.743$. The agreement between theory and experiment is quite satisfactory as far as the gross feature of IV spin response is concerned. The summed strength of IV transitions is

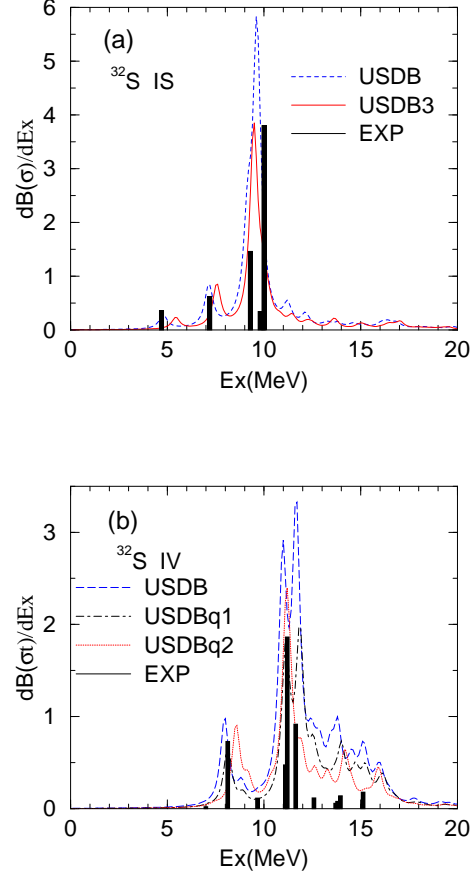


FIG. 7. (Color online) IS (top) and IV spin-M1 (bottom) transition strengths in ^{32}S . See captions to Fig. 1 for details.

$B_{exp}(\sigma\tau:Ex \leq 16\text{MeV}) = 4.120 \pm 0.407$, while the calculated results are $B_{exp}(\sigma\tau:Ex \leq 16\text{MeV}) = 7.993$. We see a large quenching for IV case with $f_s^{IV}(eff) = 0.72$. The results USDBq2 with the enhanced IS pairing and the effective IV spin operator give good account of the accumulated strength.

F. ^{36}Ar

The IS spin response in ^{36}Ar is given in Fig. 9(a). The experiments are found two states at $Ex=8.985$ and 14.482MeV with $B(\sigma) = 2.473 \pm 1.045$ and 0.872 ± 0.342 , respectively. The shell model results of USDB show a strong IS strength at $Ex=8.551\text{MeV}$ with $B(\sigma) = 1.558$. Above $Ex=10\text{MeV}$, the calculated IS strength is rather fragmented with the summed $B(\sigma) \sim 2$ in the energy region $Ex=(11-15)\text{MeV}$. The experimental summed strength in Fig. 10(a) is $B_{exp}(\sigma:Ex \leq 16\text{MeV}) = 2.910 \pm 1.091$, while the calculated value is $B_{cal}(\sigma:Ex \leq 16\text{MeV}) = 3.753$. We see a small

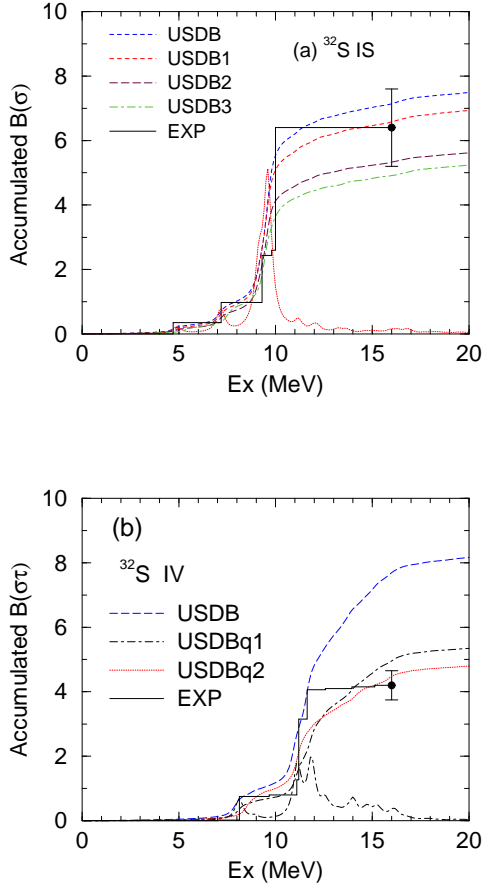


FIG. 8. (Color online) Accumulative sum of the IS spin-M1 strength (top) and the IV spin-M1 strength (bottom) as a function of the excitation energy in ^{28}Si . See the captions to Fig. 2 for details.

quenching with the factor $f_s^{IS}(\text{eff})=0.88$.

The IV spin strength is shown in Fig. 9(b). Experimental data show two large IV strength at $Ex=8$ and 10MeV having 33% and 55% of the observed total strength below $Ex=16\text{MeV}$. The calculated USDB results show also two strong spin strengths at $Ex=8.11\text{MeV}$ and $Ex=9.8\text{MeV}$ with $B(\sigma\tau)=0.648$ and 0.788 , respectively. The calculations show another strong IV transition strength with $B(\sigma\tau) \sim 2.3$ at $Ex \sim 13\text{MeV}$, while experimental data observed a small strength with $B(\sigma\tau) \sim 0.3$ around $Ex=12\text{MeV}$. The observed summed strength in Fig. 10(b) is $B_{exp}(\sigma\tau; Ex \leq 16\text{MeV}) = 1.986 \pm 0.143$, while the calculated one is $B_{cal}(\sigma\tau; Ex \leq 16\text{MeV}) = 4.125$. The quenching factor is rather large with $f_s^{IV}(\text{eff})=0.69$ for the IV case so that the results of USDBq2 in Fig. 10(b) give the closest value to the empirical one.

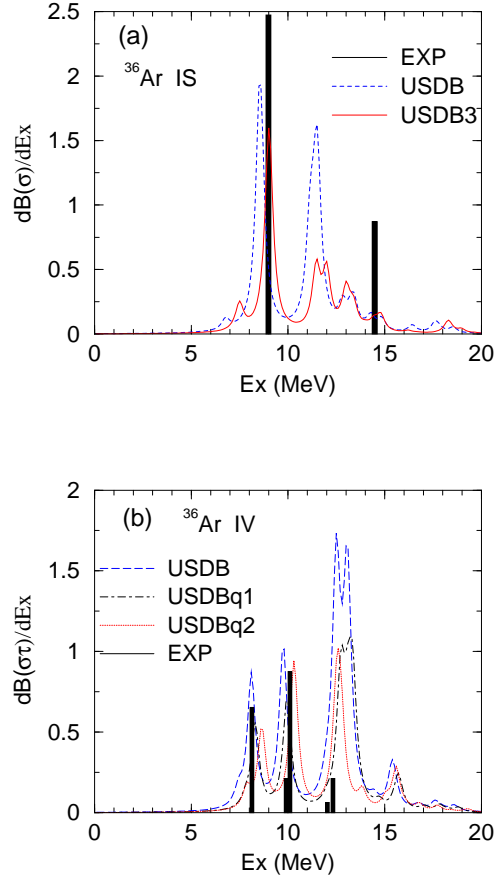


FIG. 9. (Color online) IS (top) and IV spin-M1 (bottom) transition strengths in ^{36}Ar . See captions to Fig. 1 for details.

IV. ACCUMULATED STRENGTH OF IS AND IV SPIN M1 EXCITATIONS

Figure 11 shows the sum rule values of $S(\vec{\sigma})$ and $S(\vec{\sigma}\tau_z)$ for the variations of interactions, respectively. The 10% enhanced IS pairing in USDB1 give a small quenching effect on the accumulated IS sum rule value about 5% , at most 7% in ^{32}S and ^{36}Ar . With the quenching factor $f_s^{IS} = 0.9$ in USDB2, the IS accumulated strength is further decreased by 22-25% compared with the original value by USDB interaction. The decrease of the IS summed value is going down further by the 20% enhanced IS pairing to be 29-33% in the case of USB3 results. Compared with USDB calculations, the empirical accumulated IS values are 20% enhanced in ^{24}Mg and gradually quenched from $A=28$, 0.95, 0.88 and 0.77 in ^{28}Si , ^{32}S and ^{36}Ar , respectively. In general, the quenching effect is rather small and at most 23% of the original USDB calculations with the bare spin operator.

The IV accumulated sum rule values up to $Ex=16\text{MeV}$ are shown in Fig. 11. The IS pairing interactions are

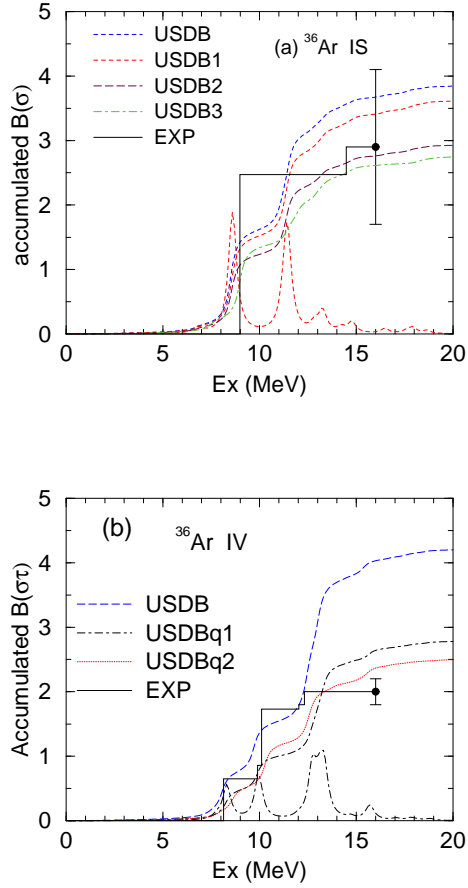


FIG. 10. (Color online) Accumulative sum of the IS spin-M1 strength (top) and the IV spin-M1 strength (bottom) as a function of the excitation energy in ^{28}Si . See the captions to Fig. 2 for details.

enhances by factors of 1.1 for USDBq1 and 1.2 for USDBq2, respectively, with the effective operators from ref. [9]. The USDBq1 results give 31-36% quenching sum rule values, while the stronger IS pairing in USDBq2 gives additional quenching of the strength, i.e., 41-45% quenching of the summed strength. The empirical values show also large quenching from 33% in ^{20}Ne , 15% in ^{24}Mg , 27% in ^{28}Si , 47% in ^{32}S and 52% in ^{36}Ar , respectively, compared with the summed value of USDB calculations.

Figure 12 shows the experimental and the calculated proton-neutron spin-spin correlations (8). Although the experimental data still have large error bars, the calculated results with the USDB interaction show poor agreement with the experimental data. This is also the case for the other USD interactions such as USD and USDA. The results with an enhanced IS spin-triplet pairing improve the agreement appreciably. For the IS channel, USDB1 adopts the bare spin operator, while the effective spin operator $f_s^{IS} = 0.9$ is used for USDB2 case. The effective operator gives a smaller spin-spin correla-

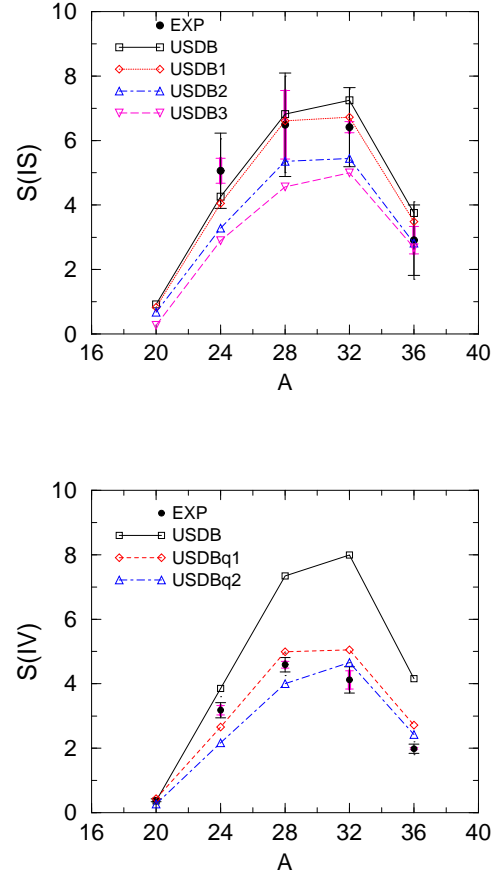


FIG. 11. (Color online) Accumulated spin-M1 transition strengths of IS channel (a) and IV channel (b). Experimental and theoretical data are summed up to $Ex = 16\text{MeV}$. Shell model calculations are performed with the USDB effective interaction: (a) In the results of USDB1 and USDB2, the IS spin-triplet pairing interaction is enhanced by multiplying the relevant matrix elements by a factor of 1.1 compared to the original USDB interactions with the quenching factor $q=1.0$ and 0.9 for IS spin operator, respectively. For USDB3, the IS pairing interaction is enhanced by a factor of 1.2 with a quenching factor $q=0.9$ for the IS spin operator. Experimental data are from ref. [20]. Long thin error bars indicate the total experimental uncertainty, while the short thick error bars denote the partial uncertainty from the spin assignment. (b) The effective IV operators are adopted for spin, orbital and spin-tensor operators. The effective operators are taken from ref. [9]. For the results of USDBq1 and USDBq2, the IS pairing interaction is enhanced by a factor of 1.1 and 1.2, respectively, with the effective operators.

tion Δ_{spin} than the case of bare IS spin operator. The positive value of the correlation indicates that the population of spin triplet pairs in the ground state is larger than that of the spin singlet pairs. We should remind that the spin and the spin-isospin M1 strength may exist in the energy region above $Ex=16\text{MeV}$. In the analysis of Figure 12, these higher energy contributions are assumed to be the same for both the IS and IV channels. In the

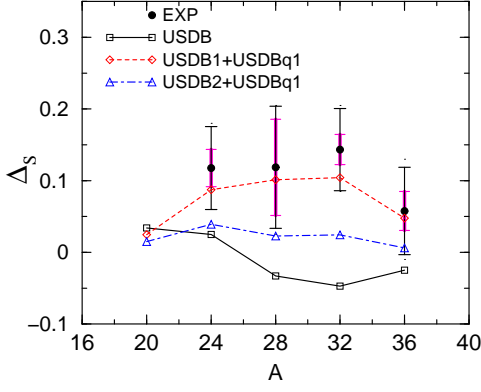


FIG. 12. (Color online) Experimental and calculated proton-neutron spin-spin correlation Δ_{spin} . Spin M1 transition strengths are summed up to $E_x=16\text{MeV}$. Shell model calculations are performed with an effective interaction USDB. In the results of USDB1 and USDB2 for the IS channel, the IS spin-triplet interaction is enhanced multiplying the relevant matrix elements by a factor of 1.1 compared to the original USDB, and the IS quenching factor is $q=1.0$ and 0.9 , respectively. The effective spin operators are used for the USDBq1 for the IV transitions. Experimental data are taken from ref. [20]. See the caption of Fig. 11 for a description of the experimental error bars.

shell model calculations in the full sd -shell, the spin M1 strength above 16MeV is small in the $N=Z$ nuclei except ^{20}Ne and ^{28}Mg . In ^{20}Ne , 20% and 51% of the total strength exist in the energy region $E_x=(16-46)\text{MeV}$ for the IS and IV channels, respectively. In the case of ^{28}Mg , the strengths above $E_x=16\text{MeV}$ are 9.9% and 21% of the total strengths for IS and IV channels, respectively. In the other nuclei, the spin strengths above $E_x=16\text{MeV}$ are rather small around few % of the accumulated strength below $E_x=16\text{MeV}$ and the strengths are more or less the same in both IS and IV channels. The hypothesis of equal IS and IV strengths in the higher energy region is valid in the present theoretical calculations in nuclei $A > 28$, which should be checked experimentally in future.

To clarify the physical mechanism of the IS spin-triplet interaction, we make a perturbative treatment of the 2-particle 2-hole (2p-2h) ground state correlations on the spin-spin matrix element. We express the wave function for the ground state with proton-neutron correlations for even-even $N=Z$ nuclei, $|\tilde{0}\rangle$, as

$$|\tilde{0}\rangle = |0\rangle + \sum_{i=1,1',2,2'} \alpha(1,1',2,2') \times |(1_\pi 1_\pi'^{-1})J_1, T_1; (2_\nu 2_\nu'^{-1})J_2, T_2 : J = T = 0\rangle. \quad (14)$$

Here the first term on the right hand side, $|0\rangle$, is the wave function with seniority $\nu = 0$ (i.e., without the spin-triplet correlations). The second term represents the states of 2 particle-hole pairs $(1_\pi 1_\pi'^{-1})$ and $(2_\nu 2_\nu'^{-1})$

for proton and neutron excitations. The indices ($i \equiv 1, 2, 1', 2'$) stand for the quantum numbers of the single-particle state $i = (n_i, l_i, j_i)$. In Eq. (14), the perturbative coefficient is given by

$$\alpha(1, 1', 2, 2') = \frac{\langle (1_\pi 1_\pi'^{-1})J_1, T_1; (2_\nu 2_\nu'^{-1})J_2, T_2 : J = T = 0 | H_p | 0 \rangle}{\Delta E} \quad (15)$$

where H_p is the IS spin-triplet two-body pairing interaction and $\Delta E = E_0 - E(11'^{-1}; 22'^{-1})$. The 2p-2h states are the seniority $\nu=4$ states in Eq. (14). The two-body matrix element in Eq. (15) is rewritten as

$$\begin{aligned} & \langle (1_\pi 1_\pi'^{-1})J_1, T_1; (2_\nu 2_\nu'^{-1})J_2, T_2 : J = T = 0 | H_p | 0 \rangle \\ &= \begin{Bmatrix} j_\pi & j_\pi' & J_1 \\ j_\nu & j_\nu' & J_2 \end{Bmatrix} \begin{Bmatrix} 1/2 & 1/2 & T_1 \\ 1/2 & 1/2 & T_2 \end{Bmatrix} \\ & \times \hat{J}_1 \hat{J}_2 \hat{T}_1 \hat{T}_2 (-)^{j_\pi + j_\nu + J_1 + J_2 + T_1 + T_2} \\ & \times \langle (1_\pi 2_\nu)J_1', T_1'; (1_\pi'^{-1} 2_\nu'^{-1})J_2', T_2' : J = T = 0 | H_p | 0 \rangle \end{aligned}$$

where $\hat{J} \equiv \sqrt{2J+1}$ and $6j$ symbols are used. The matrix element is further expressed as

$$\begin{aligned} & \langle (1_\pi 2_\nu)J_1', T_1'; (1_\pi'^{-1} 2_\nu'^{-1})J_2', T_2' : J = T = 0 | H_p | 0 \rangle \\ &= -\sqrt{2J_1+1} \langle (1_\pi 2_\nu)J_1', T_1' | H_p | (1_\pi' 2_\nu')J_2', T_2' \rangle \quad (16) \end{aligned}$$

Since the pairing interaction H_p is attractive and the energy denominator ΔE is negative, the perturbative coefficient $\alpha(1, 2, 1', 2')$ should be positive. The effect of the ground state correlations on the proton-neutron spin-spin matrix is then evaluated as

$$\begin{aligned} \langle \tilde{0} | \vec{S}_p \cdot \vec{S}_n | \tilde{0} \rangle &= 2 \sum_{1,1',2,2'} \alpha(1, 2, 1', 2') \\ & \times \langle 0 | \vec{S}_p \cdot \vec{S}_n | (1_\pi 1_\pi'^{-1})J_1, T_1; (2_\nu 2_\nu'^{-1})J_2, T_2 : J = T = 0 \rangle \quad (17) \end{aligned}$$

where the angular momenta and the isospins are selected to be $J_1 = J_2 = 1$ and $T_1 = T_2 = 0$ by the nature of the neutron-proton spin-spin matrix. The matrix element in Eq. (17) is further expressed as a reduced matrix element in the spin space,

$$\begin{aligned} & \langle 0 | \vec{S}_p \cdot \vec{S}_n | (1_\pi 1_\pi'^{-1})J_1; (2_\nu 2_\nu'^{-1})J_2 : J = 0 \rangle \\ &= \delta_{J_1, J_2} \delta_{J_1, 1} \frac{1}{\sqrt{3}} (-)^{j_1 + j_2 - j_1' - j_2' - 1} \langle j_1' || \vec{s}_p || j_1 \rangle \langle j_2' || \vec{s}_n || j_2 \rangle. \quad (18) \end{aligned}$$

In Eq.(18), the coupled angular momentum J' is taken as $J' = 1$ due to the selection rule of the spin matrix element. The isospin quantum number is discarded since it gives a trivial constant in Eq. (18). We can obtain the effect of the IS spin-triplet pairing correlations on the proton-neutron spin-spin correlation matrix element taking a 2p-2h configuration $j_1 = j_2 = j_< = 1d_{3/2}$

TABLE I. Beta-decay rate between mirror nuclei with $T = 1/2$ and $T_z = \pm 1/2$. The shell model calculations are performed by using USDB and USDB* [33] interactions with the bare spin-g factor as well as by USDBq1 and USDBq2 interactions with the Towner's effective GT operator.

A	J	USDB	USDB*	USDBq1	USDBq2	Exp.
19	1/2	2.761	2.800	2.076	2,096	1.652
21	3/2	0.486	0.514	0.372	0.398	0.323
23	3/2	0.267	0.230	0.200	0.183	0.190
25	5/2	0.616	0.661	0.515	0.539	0.414
27	5/2	0.464	0.427	0.404	0.363	0.304
29	1/2	0.233	0.180	0.194	0.154	0.176
31	1/2	0.288	0.242	0.216	0.196	0.176
33	3/2	0.171	0.156	0.135	0.127	0.0577
35	3/2	0.138	0.143	0.116	0.117	0.0505
37	3/2	0.386	0.419	0.315	0.332	0.218
σ_{rms}		0.37	0.39	0.15	0.16	

and $j'_1 = j'_2 = j_> = 1d_{5/2}$. Taking the spin-orbit splitting between $1d_{5/2}$ and $1d_{3/2}$ as 5MeV and the spin-triplet pairing matrix element as -2MeV, the α coefficient in Eq. (15) is evaluated to be 0.056. The effect on the neutron-proton spin-spin correlation becomes a large positive value, $\Delta_{spin}=0.27$. Thus, the positive value obtained by numerical results shown in Fig. 12 can be qualitatively understood by using these formulae for 2p-2h configuration mixing due to the IS spin-triplet pairing.

V. BETA-DECAY AND IS MAGNETIC MOMENTS

The effects of IS pairing and the effective spin operators are examined for the beta-decay rates between mirror nuclei with $T = 1/2$ and $T_z = \pm 1/2$. The results are given in Table I for USDB, USDB* [33], USDBq1 and USDBq2 interactions. The IS spin-triplet pairing matrix is enhanced by a factor 1.2 in the relevant matrix elements and bare spin operator is used for USDB*. The r.m.s. deviations σ_{rms} of the calculations and experiments are 0.37, 0.39, 0.15 and 0.16 for USB, USDB*, USDBq1 and USDBq2, respectively. We do not see any significant difference in the results between USDB and USDB* interactions.

Let us make the optimal χ -square fits with experimental data by using the quenching spin q factor for the bare GT operator. The r.m.s. deviation σ_{rms} of $q_{GT}(eff)^2 \times B(GT; USDB)$ from $B(GT; EXP)$ becomes the minimum value 0.030 at $q_{GT}(eff)=0.78$, while that of $q_{GT}(eff)^2 \times B(GT; USDB^*)$ from $B(GT; EXP)$ becomes the minimum value 0.039 at $q_{GT}(eff)=0.77$. We obtain more or less the same quenching factor for USDB and USDB*. This is because odd nucleon in these $T=1/2$ nuclei masks the pairing effect by the single-particle na-

ture of the transition. The r.m.s. deviations σ_{rms} get reduced for the cases with the Towner's effective operator, USDBq1 and USDBq2, though they are not as small as those for the χ -square fitted cases with the quenching factor $q_{GT}(eff)$.

The traditional source of information for the IS spin operator is from isoscalar magnetic moments, i.e., the average of the magnetic moments of mirror nuclei. The IS magnetic moments are also calculated for USDB, USDB* and USDB3 as well as for the case with Towner's effective operator (Eq. (9)) and tabulated in Table II. In case for the Towner's operator which will be denoted as 'Towner', the IS spin-triplet pairing matrix is not enhanced. The case for using the effective operator (Eq. (9)) where the coefficients are obtained by χ -square fitting the experimental isoscalar spin expectation value of sd -shell nuclei with $T = 1/2, 0$ and 1 (TABLE II of Ref. [28]). The coefficients obtained are $f_s^{IS} = 0.66$, $f_l^{IS} = 0.05$ and $f_p^{IS} = 0.06$ and the r.m.s. deviation σ_{rms} is 0.044. The results using enhanced IS spin-triplet pairing matrix by a factor 1.2 is also tabulated denoted as USDB* $_{eff}$. The σ_{rms} of the calculations and experiments shown in Table II are 0.032, 0.033, 0.030, 0.020 and 0.019 for USB, USDB*, USDB3, Towner and USDB* $_{eff}$, respectively. The results of Towner and USDB* $_{eff}$ are close to each other with smaller r.m.s. deviations and quite satisfactory. We do not see any appreciable difference among the results of USDB, USDB* and USDB3, whose r.m.s. deviations are larger but only 1.5 times those of Towner and USDB* $_{eff}$.

The IS magnetic moment is expressed by using the effective operators as [28]

$$[\mu_{IS} - J/2]/(g_s^{IS} - g_l^{IS}) = \langle J|s_z|J \rangle + g_s^{IS}/(g_s^{IS} - g_l^{IS})\delta_s \quad (19)$$

where

$$\delta_s = \delta_s \langle J|s_z|J \rangle + \delta_l \langle J|l_z|J \rangle + \delta_p \sqrt{8\pi} \langle J|[Y_2 \times \vec{s}_0^{(1)}]|J \rangle. \quad (20)$$

The effective factors δ_s , δ_l and δ_p are essentially equivalent to the effective factors in Eq. (9) as $\delta_s = f_s^{IS} - 1$, $\delta_l = f_l^{IS}/2$ and $\delta_p = f_p^{IS}$. Since the effects of spin and orbital contributions in Eq. (20) to the IS magnetic moment cancel largely because of different signs of δ_s and δ_l so that the net effect of the effective operators is rather small.

The summed IS and IV spin M1 transitions are tabulated in Table III for $N=Z$ $s-d$ shell nuclei and ^{12}C . The calculated values are obtained by the USDB and USDB* interactions with the bare spin operator as well as with the Towner's effective operators both for IS and IV transitions. The values of ^{12}C are for the IS state at $\text{Ex}=12.708\text{MeV}$ and for the IV one at $\text{Ex}=15.113\text{MeV}$, respectively. For the summed strength, the enhanced IS interaction USDB* gives 12-18% quenching for the IS spin transitions and 18-24% quenching for the IV ones except ^{20}Ne (38% for IS and 40% for IV). The different values between ^{20}Ne and the other nuclei is due to the smaller summed values below $\text{Ex}=16\text{MeV}$ for ^{20}Ne , which exhaust only 80% and half of the total strength

TABLE II. IS magnetic moments extracted from the average of magnetic moments in mirror nuclei. The shell model calculations are performed by using USDB, USDB* and USDB3 interactions as well as for the case with the Towner's effective operator (denoted as Towner). The case with the effective operator (Eq. (9)) where the coefficients are obtained by chi-square fitting procedure (denoted as USDB*_{eff}) is also given. The values are given in a unit of nuclear magneton μ_N

A	J	USDB	USDB*	USDB3	Towner	USDB* _{eff}	Exp.
19	1/2	0.431	0.432	0.414	0.385	0.371	0.371
21	3/2	0.869	0.870	0.858	0.850	0.853	0.862
23	3/2	0.844	0.838	0.829	0.832	0.834	—
25	5/2	1.403	1.403	1.388	1.384	1.397	1.395
27	5/2	1.388	1.381	1.368	1.373	1.384	1.393
29	1/2	0.315	0.304	0.298	0.301	0.297	0.340
31	1/2	0.323	0.313	0.307	0.307	0.302	0.322
33	3/2	0.691	0.676	0.683	0.711	0.722	—
35	3/2	0.676	0.679	0.686	0.715	0.724	0.727
37	3/2	0.629	0.630	0.642	0.681	0.692	—
σ_{rms}		0.032	0.033	0.030	0.020	0.019	

of full model space for IS and IV channels, respectively, while more than 90% of the total strength exists below $Ex=16\text{MeV}$ in other nuclei (except IV channel of ^{28}Mg ; 80%). The Towner's effective operators give large quenched values, about 47-48% quenching for all nuclei in the IS channel and 27-28% quenching (21% for ^{20}Ne) for the IV one. The experimental summed values of the IS strengths show rather minor quenching or even enhanced in ^{24}Mg compared with USDB results, while the IV data show a large quenching consistent with those obtained by Towner's effective operators. More quantitatively, we need a combined effect of the enhanced IS pairing and the effective operators to get better agreement with the experimental values of IV channel for $A \geq 28$ as seen in Fig. 11. Although the IS moments are very well described by Towner and USDB*_{eff}, the calculated $S(IS)$ values prove to be much suppressed compared with the experimental data. The values of accumulated strengths $S(IS)$ are 0.485 (0.318), 2.221 (1.520), 3.579 (2.356), 3.810 (2.490) and 1.975 (1.282) for ^{20}Ne , ^{24}Mg , ^{28}Si , ^{32}S and ^{36}Ar , respectively, for Towner's operators (USDB*_{eff}).

The difference between the IS magnetic moment and the spin M1 transition will be clarified by the following way. The IS spin M1 transition is expressed as

$$\langle J|\hat{O}(\sigma)|0\rangle = (f_s^{IS} - f_l^{IS})\langle J|\vec{\sigma}|0\rangle + f_g^{IS}\sqrt{8\pi}\langle J|[Y_2 \times \vec{\sigma}]^{(1)}|0\rangle \quad (21)$$

where the non-diagonal matrix element of the operator \vec{J} vanishes, and the effective operators f_s and f_l have different signs so that the net effect gives a large quenching

effect. This is rather different from the IS magnetic moment in Eq. (19) where the effects of effective spin and orbital operators cancel largely.

VI. SUMMARY

In summary, we studied the IS and IV spin M1 transitions in even-even $N=Z$ sd -shell nuclei using shell model calculations with USDB interactions in full sd -shell model space. We introduced the effective operators for the spin and spin-isospin M1 operators in Eqs. (9) and (11) as well as the enhanced IS spin-triplet pairing. In general, the calculated results show good agreement with the experimental energy spectra in $N=Z$ nuclei as far as the excitation energies are concerned. Compared with the experimental M1 results, the accumulated IS spin strengths up to 16MeV show small quenching effect, corresponding to the effective quenching operator $q^{IS}(eff) \sim 0.9$, while a large quenching $q^{IV}(eff) \sim 0.7$ is extracted for the IV channel. The similar quenching on the IS spin M1 transitions is obtained by the 20% enhanced IS spin-triplet pairing correlations with the bare spin operator. The enhanced IS pairing does not change much the excitation energy spectra themselves. Positive contributions for the spin-spin correlations are found by an enhanced isoscalar spin-triplet pairing interaction in these sd -shell nuclei. The effects of the effective spin operators and enhanced IS pairing is also examined on the beta decay rate and the IS magnetic moments in sd -shell nuclei. The r.m.s. deviation between the calculations and experiments of beta decay rate are improved by the effective operator, while the IS pairing has only a minor effect on these observables since the unpaired particle masks the effect of pairing correlations on the matrix elements.

The Towner's effective spin operators works well to reproduce the accumulated experimental IV spin strength, while the quenching of the effective operators is much larger than the observed one in the IS spin channel. In the past, a large quenching of IS magnetic transition strength was suggested in the literatures. However, the (p,p') data in ref. [20] do not show any sign of the large quenching effect on the IS spin transitions. This point should be studied further experimentally by possible IS probes such as (d,d') reactions [34] together with comprehensive theoretical calculations.

ACKNOWLEDGMENTS

We would like to thank H. Matsubara for providing the experimental data. We would also like to thank M. Ichimura, A. Tamii, M. Sasano and T. Uesaka for the useful discussions. This work was supported in part by JSPS KAKENHI Grant Numbers JP16K05367 and JP15K05090.

TABLE III. Summed IS and IV spin M1 transitions in $s - d$ shell nuclei and ^{12}C . Calculated and experimental values are accumulated up to $E_x=16\text{MeV}$. The shell model calculations are performed by using USDB and USDB*(the IS pairing is enhanced) interactions as well as for the case with the Towner's effective operator (denoted as Towner) for USDB results. For ^{12}C , the shell model calculations are performed with SFO interaction with the bare spin operator. The experimental IS strength is for the state at $E_x=12.708\text{MeV}$, while the IV strength is for the state at $E_x=15.113\text{MeV}$. Experimental data are taken from ref. [20]. The values in the bracket are experimental errors.

A	S(IS)				S(IV)			
	USDB	USDB*	Towner	Exp.	USDB	USDB*	Towner	Exp.
^{20}Ne	0.919	0.574	0.485	—	0.577	0.346	0.456	0.387 (0.042)
^{24}Mg	4.256	3.573	2.221	5.05 (1.00)	3.856	2.937	2.808	3.3 (0.3)
^{28}Si	6.816	5.632	3.579	6.5 (1.5)	7.340	5.593	5.256	4.6 (0.35)
^{32}S	7.247	6.167	3.810	6.4 (1.2)	7.993	6.554	5.734	4.2 (0.45)
^{36}Ar	3.753	3.303	1.975	2.9 (1.1)	4.159	3.414	2.978	2.0 (0.2)
^{12}C	1.516	—	—	3.174(0.842)	1.937	—	—	1.909 (0.094)

- [1] A. Bohr and B. R. Mottelson, *Nuclear Structure* (World Scientific, 1969), Vol. I.
- [2] C. Gaarde et al., Nucl. Phys. A369 258 (1981).
- [3] T. Wakasa et al., Phys. Rev. C 55, 2909 (1997).
- [4] K. Yako et al., Phys. Lett. B615, 193(2005).
- [5] K. Yako et al., Phys. Rev. Lett. 103, 012503 (2009).
- [6] M. Sasano, *et al.*, Phys. Rev. Lett. 107, 202501 (2011); M. Sasano et al., Phys. Rev. C86, 034324 (2012).
- [7] T. Wakasa et al., Phys. Rev. C 85, 064606 (2012).
- [8] A. Arima, K. Shimizu, W. Bentz and H. Hyuga, Adv. Nucl. Phys. 18, 1 (1987).
- [9] I. S. Towner, Phys. Rep. 155, 263 (1987).
- [10] K. Langanke et al., Phys. Rev. Lett. 93, 202501 (2004); 100, 011101 (2008).
- [11] S. Reddy et al., Phys. Rev. C59, 2888(1999); A. Burrows and R. F. Sawyer, Phys. Rev. C58, 554 (1998).
- [12] S. Fantoni et al., Phys. Rev. Lett. 87, 181101 (2001); G. Shen et al., Phys. Rev. C87, 025802 (2013).
- [13] A. Radhi et al., Phys. Rev. C91, 045803(2015).
- [14] G. Bertsch and I. Hamamoto, Phys. Rev. C26, 1323(1982).
- [15] A. Bohr and B. R. Mottelson, Phys. Lett. 100B, 10 (1981).
- [16] M. Rho, Nucl. Phys. A 231, 493 (1974); E. Oset and M. Rho, Phys. Rev. Lett. 42, 47 (1979).
- [17] A. Arima, in *Proceedings of the International Symposium on New Facet of Spin Giant Resonances in Nuclei, 1997*, edited by H. Sakai, H. Okamura, and T. Wakasa (Univ. of Tokyo, Japan, 1997), p. 3.
- [18] M. Ichimura, H. Sakai and Wakasa, Prog. Part. Nucl. Phys. 56, 446 (2006).
- [19] W. A. Richter, S. Mkhize and B. A. Brown, Phys. Rev. C78, 064302 (2008).
- [20] H. Matsubara et al., Phys. Rev. Lett.115, 102501 (2015) and private communications.
- [21] C.L. Bai, H. Sagawa, M. Sasano, T. Uesaka, K. Hagino, H.Q. Zhang, X.Z. Zhang, and F.R. Xu, Phys. Lett. B719, 116 (2013).
- [22] H. Sagawa, C.L. Bai and G. Colò, (2016) Physica Scripta the '75 Nobel Prize celebration volume(2016) in press.
- [23] Y. Fujita *et al.*, Phys. Rev. Lett. 112, 112502 (2014).
- [24] Y. Tanimura, H. Sagawa and K. Hagino, Prog. Theor. Exp. Phys. 053D02 (2014).
- [25] S. J. Q. Robinson and L. Zamick, Phys. Rev. C66, 034303 (2002).
- [26] B. A. Brown and W. A. Richter, Phys. Rev. C74, 034315 (2006).
- [27] B. H. Wildenthal, Prog. Part. Nucl. Phys. 11, 5 (1984); B. A. Brown and B. H. Wildenthal, Annu. Rev. Nucl. Part. Sci. 38, 29 (1988).
- [28] B. A. Brown and B. H. Wildenthal, Phys. Rev. C28, 2397 (1983).
- [29] P. von Neumann-Cosel et. al., Nucl. Phys. A669, 3 (2000).
- [30] T. Suzuki, R. Fujimoto and T. Otsuka, Phys. Rev. C67, 044302 (2003).
- [31] J. B. Flanz et al., Phys. Rev. Lett. 43, 1922 (1979).
- [32] C. D. Hoyle et al., Phys. Rev. C27, 1244 (1983).
- [33] H. Sagawa, T. Suzuki and M. Sasano, Phys. Rev. C94, 041303(R) (2016).
- [34] T. Kawabata et al., Phys. Rev. C70, 034308 (2004).